

## Assessment of Ras El Ma Karst Spring Features by Structural and Functional Approaches at the Region of Taza, Morocco

Jamal Naoura<sup>1\*</sup>, Imad El Kati<sup>1</sup>, Lahcen Benaabidate<sup>2</sup>

<sup>1</sup> Laboratory of Natural Resources and Environment, Polydisciplinary Faculty, University of Sidi Mohammed Ben Abdellah, Taza 35000, Morocco

<sup>2</sup> Laboratory of Functional Ecology and Environment Engineering, Faculty of Sciences and Techniques, University of Sidi Mohammed Ben Abdellah, Fes 30000, Morocco

\* Corresponding author's e-mail: jamal.naoura@usmba.ac.ma

### ABSTRACT

This work performed by considering two complementary approaches for investigating the Karst system of Ras El Ma source: (1) The structural approach based on field studies, (2) The functional approach requiring inputs data (precipitations) as well as output data at the exit of the karstic system. The choice of the Ras El Ma source is justified by the fact that it constitutes the main outlet of the Liassic aquifer at the Southwest of Taza town. The structural approach highlighted that the impact of South Rifan and North Middle Atlas faults, oriented mainly NE-SW to ENE-WSW and NW-SE, tectonically linked to the Hercynian and late-Hercynian phases; these faults compartmentalized the karst into panels. The functioning of this karst system is based on the coupling of inputs and outputs, the analysis of interannual hydrograph, flood hydrographs, the recession curves and the analysis of hydro-geochemical results. Respectively, the obtained results are presented as follows: A close relationship between flow rates and precipitation, interannual hydrographs marked by a contrasting variation in flow rates and a periodicity that occurs between low water and high-water years. Concerning flood hydrographs, there are two types, a unit modal hydrographs type which generally occurs following time concentrated rainfall and a second multi modal hydrographs type which follows the repetitive rainfall in the basin. The study of recession curves reveals a clear complexity of the systems supplying the source. However, due to the low drying-off coefficients ( $7.66 \cdot 10^{-4}$ ), the aquifer seems to have a poorly developed drainage network in a flooded area. According to the Mangin method [1975], this karstic system is classified in the category of poor or complex karst systems taking into accounts two parameters (i) and (K), which characterize the functioning of the infiltration zone and the volume of flooded karst, respectively. The physicochemical parameters study highlighted the nature of drained rock by the sources. The correlation between conductivity and different chemical elements shows that bicarbonates and calcium are responsible for the mineralization of the waters of this source. It can be concluded that the low values of mineralization occur during the winter and spring floods. The spring regains its normal mineralization during the summer period.

**Keywords:** Karst aquifers, hydrogeological functioning, Ras El Ma spring, model of Mangin, Morocco.

### INTRODUCTION

Karst aquifers are typically characterized by great heterogeneity due to their irregular pore network, cracks, fractures and conduits of very different shapes, sizes and connections, which make these systems unique and different from other aquifers [Bakalowicz, 2008 in Paiva and Cunha, 2020].

Depending on the development level of the channel network and its interconnection within

the karst system, it is possible to define two types of karst aquifers [White, 1988; Ford and Williams, 2007; Taylor and Greene, 2008]. A karst system is characterized by a well-developed and well-organized network of karst conduits, which allows drainage after rainfall due to the high transmissivity and low storage capacity. This results in an intense discharge over a short period characterized by a peak flow on the flood hydrograph. These aquifers are known as fast-flowing

or fast-flowing karst systems. Conversely, diffuse karst is a system which differs from the first type by the predominance of base flow instead of rapid flow. In this type of karst system, the conduit network is poorly developed or poorly interconnected; thus, water takes a long time to transit from the recharge area to the outlet. These diffuse karst aquifers hold water for a much longer period; moreover, they have a high capacity to store it, and release it later in a dry period or season. Consequently, the hydrogeological study of karst aquifers by classical study methods, such as the application of Darcy's law, pumping tests and mesh models, is particularly difficult or even impossible [White, 1988; Ford and Williams, 2007; Goldscheider and Drew, 2007; Andreo et al., 2008; Kresic et al., 2010; Fiorillo, 2014; Mikszewski and Kresic, 2015]. Presently, karst hydrogeologists use a specific study methodology to provide the information on different types of flow, groundwater circulation routes, storage capacity and spatial and temporal variations [Goldscheider and Drew, 2007; Taylor and Greene, 2008]. Detailed work on karst hydrodynamic investigation methods was presented by several authors [Bakalowicz, 2005; Kovács et al., 2005; Ford and Williams, 2007; Taylor and Greene, 2008; Martinez-Santos and Andreu, 2010; Rehr and Birk, 2010; Kresic and Stevanovic, 2010; Ghasemizadeh et al., 2012; 2013; Hartmann et al., 2014].

Over the last decades, some authors focused on the following topics: the analysis of time series which are vectors for interesting information on the complex input-output relationship inside karst aquifers [Labat et al., 2000; Rahnemaei et al., 2005; Panagopoulos and Lambrakis, 2006; Gárfias-Soliz et al., 2010; Jukić and Denić-Jukić, 2011]; the study of recession curves widely applied as a useful tool for understanding the aquifer hydrodynamics and physical characteristics [Mangin, 1975; Bonacci, 1993; Kovács et al., 2005; Florea and Vacher, 2006; Fiorillo, 2011; Malík and Vojtková, 2012; Chang et al., 2015]; the analysis of physicochemical and isotopic temporal variations of the water of the karst outlets allows determining the directions, the paths and the velocities of the flows as well as the storage in the karstic aquifer [Anderson, 2005; Luhmann, 2011]. Some authors have used water temperature and conductivity separately or in combination to understand the hydrodynamics and structural organization of drainage in the karst system [Massey et al., 2007; Liñan et al., 2009; Wang et al.,

2009; Wang et al., 2019, Paiva and Cunha, 2020]. When studying karst, scientists widely appreciate the combination of hydrodynamic and physicochemical analyses, especially of spring flows [Birk et al., 2004; Liu et al., 2010; Luhmann et al., 2012; Mudarra et al., 2014; Sánchez et al., 2015; Bicalho et al., 2017; Petalas et al., 2018; Gil-Márquez et al., 2019].

The present research aimed to apply a methodology combining two approaches which are widely used in investigating the karst hydrogeological functioning. A structural approach is used to identify the fracture network and preferred flow directions from field data. Furthermore, the functional approach was used to highlight the hydrodynamic behavior of the karst aquifer from the output data of this system; flow rates and water physicochemical characteristics.

### Overview of study area

The study area (Fig. 1) is presented as one of the most important regions of Morocco regarding karstic aquifers. It therefore deserves to be studied. This area roughly encompasses the mountainous region south of Taza town. By its southern position, between the Middle Atlas foothills and the pre-Rif sector, this area offers the character of a contrasting mountain region with a presence of plateaus, hills and plains [Rachid, 1997]. Previous geological and hydro-stratigraphic studies showed a lithological variation in deep and at outcropping formations, occupied by Paleozoic schists and Triassic clay formations with low permeability, respectively, overlaid or juxtaposed by the permeable Liassic carbonate formations [Colo, 1961; Mathieu, 1964; Benshili, 1989; Laville et Faden, 1989; Sabaoui et viallard 1998 ; Auajjar et Boulegue, 1999; Laville et al., 2004], which constitute the potentials stratified aquifers: the dolomitic aquifer of the Lower Liassic, the aquifer of slab limestones and clayey limestones of the Middle Liassic, the aquifer of sandstone limestones at the base of the Miocene and the aquifer of Quaternary limestones. These carbonate formations have numerous superficial karstic faces (Polje, Lapiez, Ponor, Aven, Doline...) and underground where the most important is Friouatto cave.

The climatology of the study area is characterized by highly fluctuating precipitation, contrasted by orography and hydrological cycles. The average cumulative annual rainfall is around 560 mm, but the South part of the study area is

characterized by fairly high altitudes (1500 to 2000 m) allowing winter humidity of more than 1000 mm/year on average at the Bab Boudir station. The average seasonal rainfall of 265 mm showed that winter is the rainiest season, while summer is drier with less than 3 mm, Autumn is rainier than spring but with less important averages. The average monthly rainfall is 39.50 mm. January, February and March are the wettest months, while July receives the weakest water budget. For temperatures, January and February are the coldest months while August is the hottest month. The annual average temperature is 19.57 °C. The actual evaporation evaluated by Turc and Thornthwaite methods gave an average value of 400 mm. However, this value remains lower than the average annual rainfall (560 mm). The resulting surplus contributes to supplying groundwater, in particular the Liassic limestones and/or surface runoff [Naoura, 2012].

## MATERIALS AND METHODS

Unlike porous media, karst presents different flow conditions. Indeed, karstification by prioritizing flows, introduces heterogeneity at all observation levels [Mangin, 1975; Bakalowicz, 1979]. Thus, for this reason and previous reasons mentioned in the introduction, the use of suitable methods for porous media will not provide for karst aquifers the results compatible with reality in most cases.

In the present study, the Ras El Ma and Laanaceur karst aquifer is considered as a black box, due to the scarcity of information from the previous scientific studies concerning: (1) the geographical extent and the limit between the different hydrogeological panels as well as possible communications, (2) data time series (inputs / outputs), (3) internal characteristics of the aquifer.

In order to achieve a preliminary understanding of the functioning of the Ras El Ma and

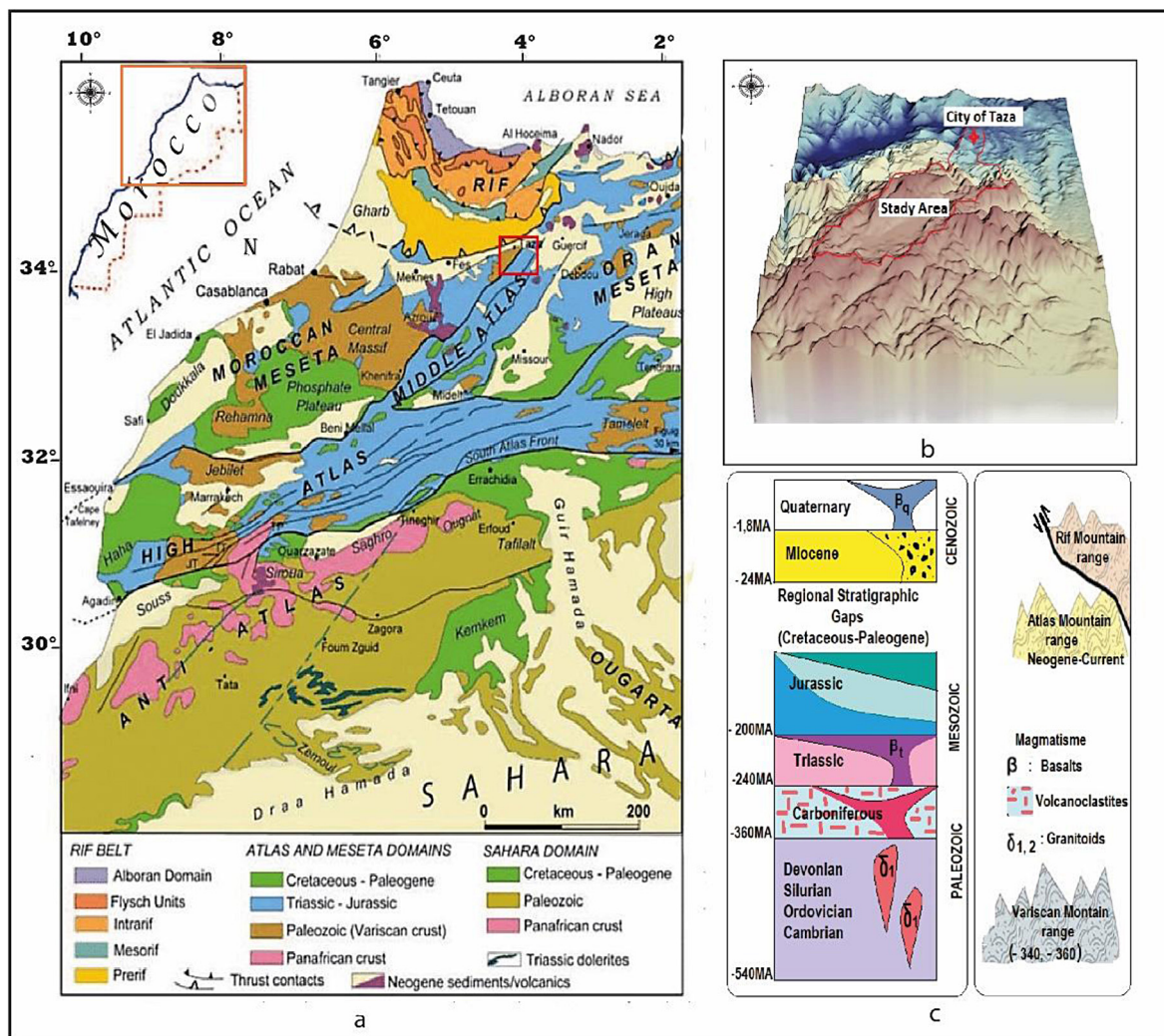


**Figure 1.** Location map and characteristics of the study area; a) Location map of the study area (modified after [Frizon de Lamotte et al., 2004]; b) MNT of the study area; c) Stratigraphy and paleogeography of the study area

Laanaceur karst aquifers, a synthesis of the factors influencing surface runoff and depth flow in the study area is necessary (lithology, tectonics, permeability and slopes). Subsequently the following approached: (1) analysis of the flow chronological series, (2) analysis of the recession curves (recession curves), (3) analysis and interpretation of water hydrogeochemical results in the source Ras El Ma.

The study was based on flow chronological series obtained from the Sebou Hydraulic Basin Agency (ABHS), spanning a period of 31 years (10/03/1989 - 03/07/2020) which appears reasonable to draw reliable conclusions. Furthermore, the hydrogeochemical analyses were carried out in the Laboratory of Natural Resources and Environment (RNE) during the year 2017. At the weekly to bimonthly time step, sampling is representative of seasonal variations and provides a satisfactory estimate of the variations in temperature and water chemistry during a cycle. The hydrogeochemical method is not as simple and generalized for all karst systems, so the choice of markers will be imposed by the type of information sought and the means available. The physical parameters were analyzed. The conductivity measured in situ with a portable conductivity meter the values of which are given in ( $\mu\text{s}/\text{cm}$ ). The measurements in the field were reduced to 20 °C by the formula of J. Rodier [1980]:

$$\text{Cond}20^\circ = \frac{Ct}{0.0227 * t - 0.56}$$

where:  $Ct$  – Conductivity and  $t$  – temperature of water measured in situ using a 1/10 ° mercury thermometer.

These two markers will provide crucial information on the functioning (development and organization of the karstification within the system).

The pH measured either in the field or in the laboratory using an electric pH meter accurate to within 1/10<sup>th</sup> pH unit. This marker conditions the physicochemical equilibrium, in particular the calco-carbonic equilibrium and thus the action of the water on the carbonates (attack or deposit). The pH is acidic in the waters of sandy or granitic aquifers. It is alkaline in limestone.

Major elements:  $\text{Ca}^{2+}$ ,  $\text{Mg}^{2+}$ ,  $\text{Na}^+$  and  $\text{K}^+$ ,  $\text{HCO}_3^-$ ,  $\text{Cl}^-$ ,  $\text{SO}_4^{2-}$  and  $\text{NO}_3^-$  were also analyzed. Three methods were used to perform the determinations of these elements: (1) volumetric determination of calcium with EDTA acid, bicarbonates

with sulfuric acid, chlorides with mercuric nitrate and magnesium by EDT; (2) spectrophotometry for sulfates and nitrates; (3) flame spectrophotometry for sodium and potassium. These markers allow estimating the residence time of the water in the system, informing on the modalities of infiltration and detecting the possibilities of mixing of waters of different origins.

## RESULTS AND DISCUSSIONS

### Structural approach

#### *Study of the factors influencing surface runoff and flow in the study area*

The establishment of the permeability map of the study area was based on the hypsometric, lithological and structural nature. Thus, permeability divided into four classes was found by combining these three parameters (Fig. 2a). In the study area, despite the hypsometric distribution into seven classes (Fig. 2b), two areas can easily be distinguished: in its southern part, the Chiker's polje, which is a vast flat-bottomed depression closed by steep rocky slopes (steep slopes). Despite the diversity of the lithological formations outcropping in the study area (Fig. 2c), its geomorphology as well as its hydrological behavior are closely linked to the Middle Atlas domain characterized by essentially carbonate formations which constitute a highly developed karst system thus, conditioning a high permeability. Occasionally, the outcrops of some gray and brown marl passage, of the Upper Domerian - Toarcian or alluvial deposits, give semi-permeable or even impermeable formations.

This formation is characteristic of karstic environments. The waters are drained by the ponor called the ponor of Assoukh. This latter feeds the karstic water table which essentially produces the resurgence of Ras El Ma which is at the origin of the river of Taza stream. In the Northern part, the hypsometric characteristics subsequently become average to weak.

The structural environment of the study area (Fig. 3) has never undergone significant tectonic movements after the Hercynian phases. The major Hercynian accidents are reactivated during Meso-Cenozoic times and guided the structuring of the Middle Atlas. According to the geological map of Taza, the major accident is the ANMA (North Middle Atlas Accident) which played an important tectonic role. It separates this part of

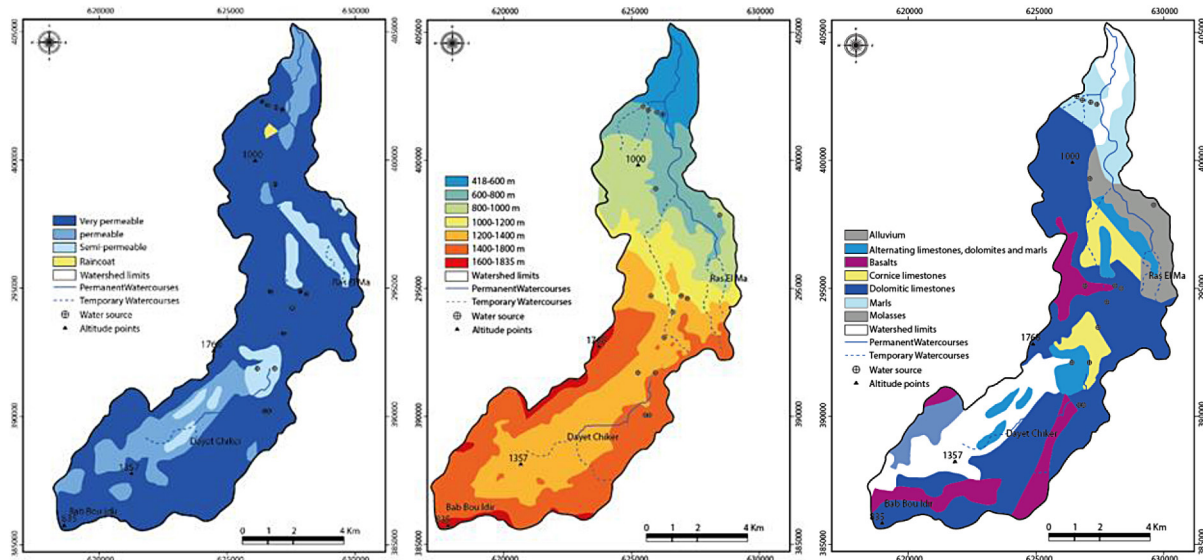


**Figure 2.** Map of the factors influencing surface runoff and flow in the study area; a) Map of permeability; b) Map of hypsometric; c) Map of lithology

the Middle Atlas into two zones, one tabular in the west and the other folded in the east. Several folds (anticlinal wrinkles and synclinal depressions) distort the Middle Atlas. They are generally oriented NE-SW or N-E and are cut or sometimes chopped by longitudinal and transverse fractures [Ramirez et al., 2008].

Among the NE-SW folds there are: The anticline of Jbel Bou Messaoud and the synclinal of Daya Chiker, in addition to anticlines and synclines of lesser magnitude of variable axial direction are grafted between the flanks of these two major folds. For the N-E folds there are the wrinkle, of Rouis el Guendour, anticlinal ridge of Bab Boudir. The secondary cover of the folded and tabular Middle Atlas in the study area is crossed by three fracture systems that were mapped in the Taza sheet and by various authors such as [Colo, 1961; Robillard 1981; Sebaoui, 1998].

A dominant longitudinal system, is formed by faults oriented between N20 and N60, subvertical. A transverse system, is formed by faults oriented between N120 and N170, subvertical. They generally shift the longitudinal system in dextral and sinister. A system of faults of lesser importance, subequatorial, oriented between N90 and N100, locally affects the secondary formations of the Middle Atlas. Under the effect of the South Rifain and North Middle Atlas tectonic accidents, oriented mainly NE-SW to ENE-WSW and NW-SE and tectonically linked to the Hercynian and late-Hercynian phases [Combe, 1971; Robillard, 1977; Sebaoui, 1998], this

series was compartmentalized into panels [ABHS, 1995]: Moukda and Magoussa panel, Ras El Ma and Aanaceur panel and the NE panel of the town of Taza.

These tectonic accidents become preferential outlets for groundwater circulation and appear as very frequent springs which generally emerge from the base of limestone beds in contact with marls or clays (Triassic in general). Their significant flows vary rapidly, which characterizes the karst sources (sources with immediate response) such as the Ras El Ma spring .

## Functional approach

### Study of flows variation of the Ras El Ma spring

For this study, the authors employed the flow data of the Ras El Ma spring over a period of 31 years (10/03/1989- 03/07/2020) as well as a chronicle of precipitation in the region. The relationship between inflows and outflows (flow and ETR) is illustrated by Figure (4). Globally, the variations in flows of this spring are closely linked to irregularities in precipitation, but the response is delayed under the effect of the recharge of the karstic aquifer, especially during the autumn season, something which will be verified later with the results of recession curves. The maximum flow is recorded in the middle of winter followed by a return to slowing down following fluctuations in precipitation.

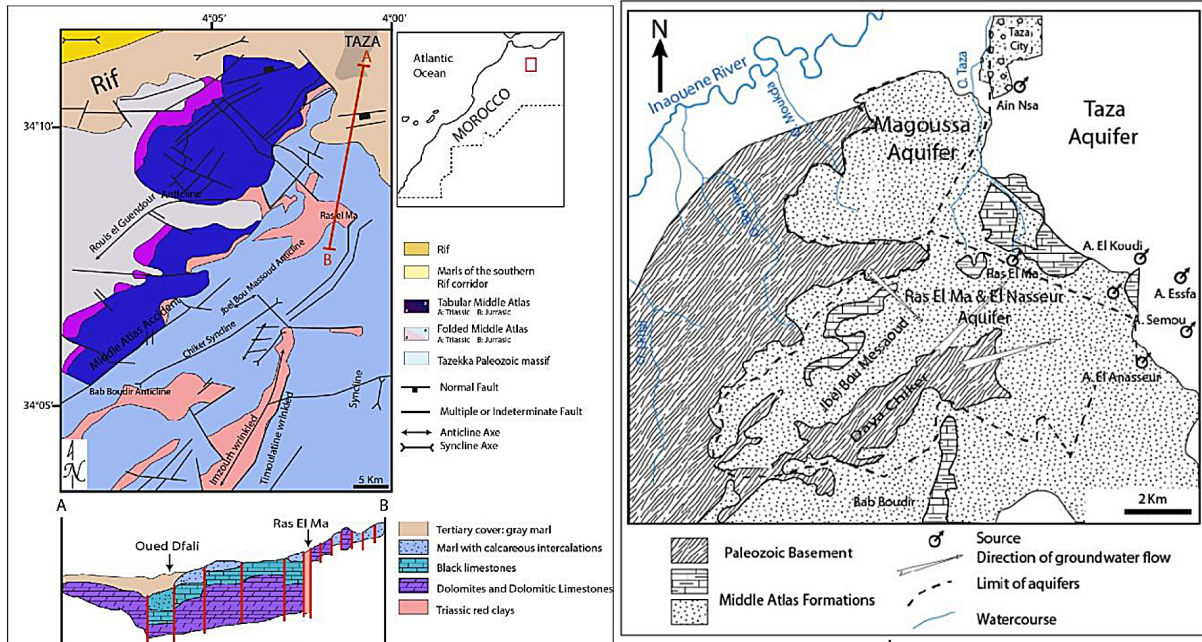


**Figure 3.** Structural environment of the study area modified; a) Structural map and geological section (Ramirez et al. 2008); b) Schematic map of the aquifers (ABHS.1995)

The average annual flow from this source is around  $350 \text{ L}\cdot\text{s}^{-1}$ . Figure (5) also shows that the flow rates from this source can reach up to  $800 \text{ L}\cdot\text{s}^{-1}$  during the periods of high water. Furthermore, in the periods of low water, this source does not exceed  $25 \text{ L}\cdot\text{s}^{-1}$ . The striking effect for this chronicle is the extreme situation, recorded on 12/26/1990 with a flow rate of  $2490 \text{ L}\cdot\text{s}^{-1}$  following exceptional humidity met during this year. Another remark concerning the hydrograph of this source is the cyclicity

which occurs between the years of low water (generally period of 3 years) and cycles of high water (generally of 2 years).

### Study of flood hydrograph curves

The different floods of the Ras El Ma spring generally present two types of hydrographs (Fig. 6): (1) Classic unit hydrographs (floods of 1995, 2001, 2007, 2013 and 2014), with an individualized high peak flow, a generally very short rise

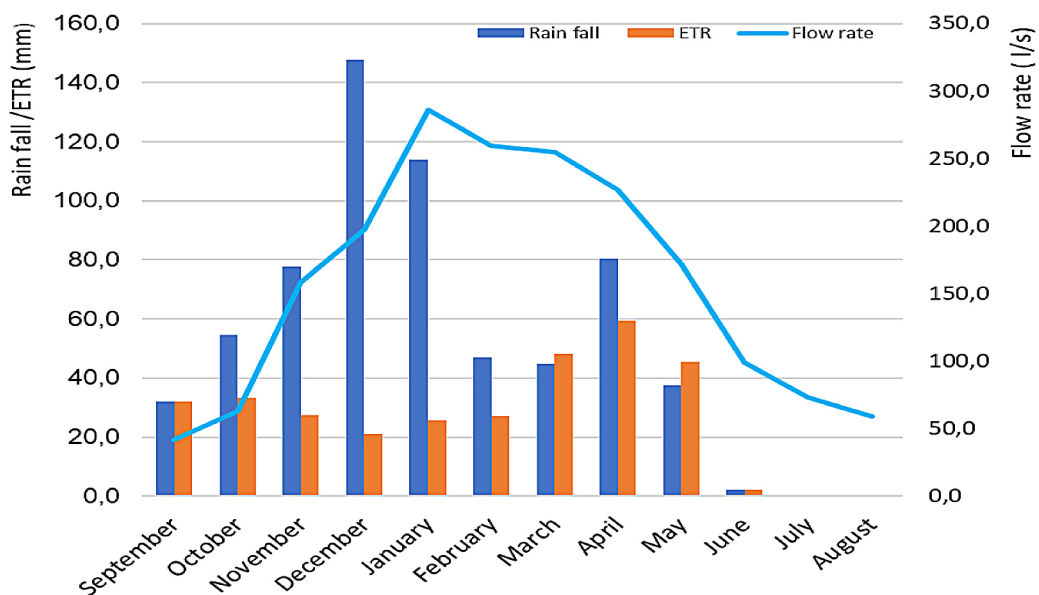


**Figure 4.** Relation between inflows and outflows (flow and ETR)

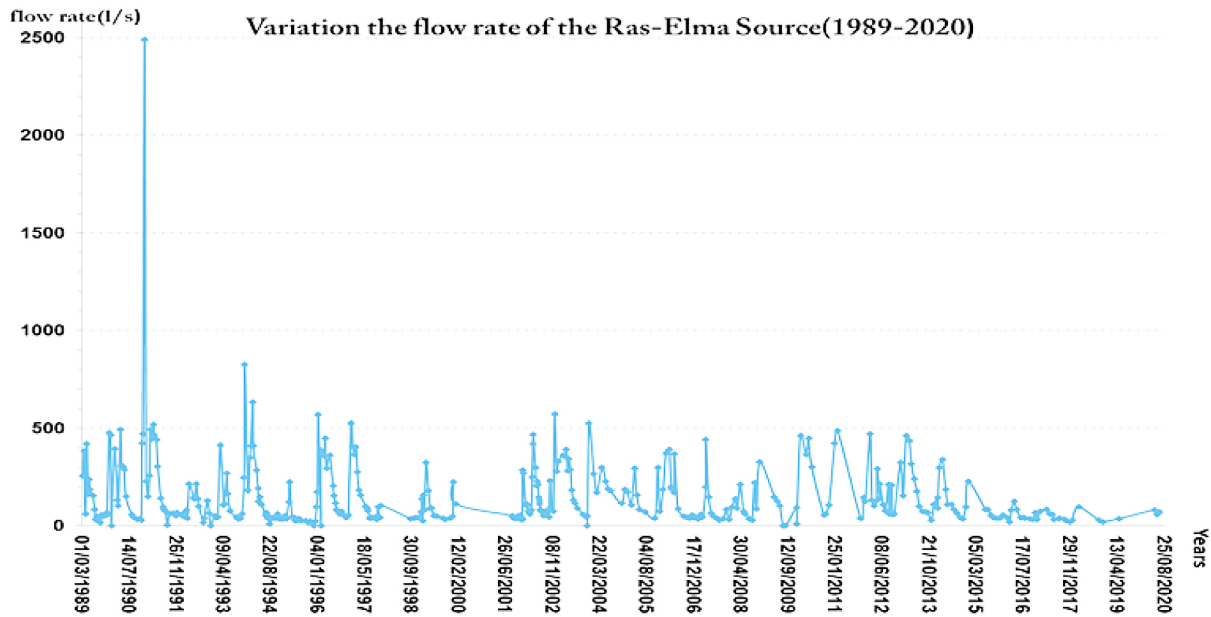


Figure 5. Flow variation of the Ras El Ma Spring (1994-2004)

time, and finally a longer fall time, followed by drying up. These floods are generally due to heavy uniform rains of short duration over the entire upstream basin of the spring. (2) Very frequent hydrographs characterized by a succession of rises without clearly visible peak (Floods of 1989, 1996, 2000 and 2002). They are due to the influx of successive masses of water in response to separate rainfall events.

*Study of recession curves*

The study of flow chronological series is essential to understand the evolution and the interaction between the inputs and the outputs of a karst system. However, to fully understand the internal hydrodynamic functioning of this system, it is necessary to refer to the recession curves, the main ones of which are illustrated in Figure (7)

This method, introduced by Mangin [1975], allows quantitatively characterizing the infiltration conditions throughout the unsaturated zone and the storage capacity of the saturated zone. The method consists of modeling the recession curves using a model with two mathematical functions, each representing two reservoirs independent of each other. These two conceptual reservoirs are the infiltration zone and the flooded zone.

The recession curve of 03/09/2001 was taken as a reference given its representative quality and the chronicle of its follow-up (Fig. 8). It should be noted that the various other recession curves (Fig. 7) show very variable trends, which leaves us very cautious about their uses, given their very large measurement step.

Thus, the function  $\psi(t)$  represents the function of the recession curve which corresponds to the emptying of the infiltration zone (unsaturated

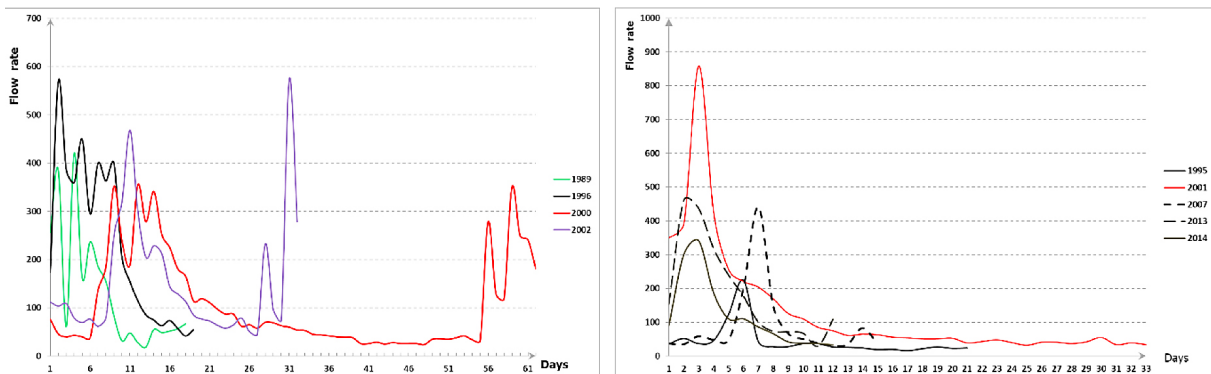


Figure 6. Flood hydrographs types of Ras El Ma Spring; a) unit hydrographs; b) multi-modal hydrographs

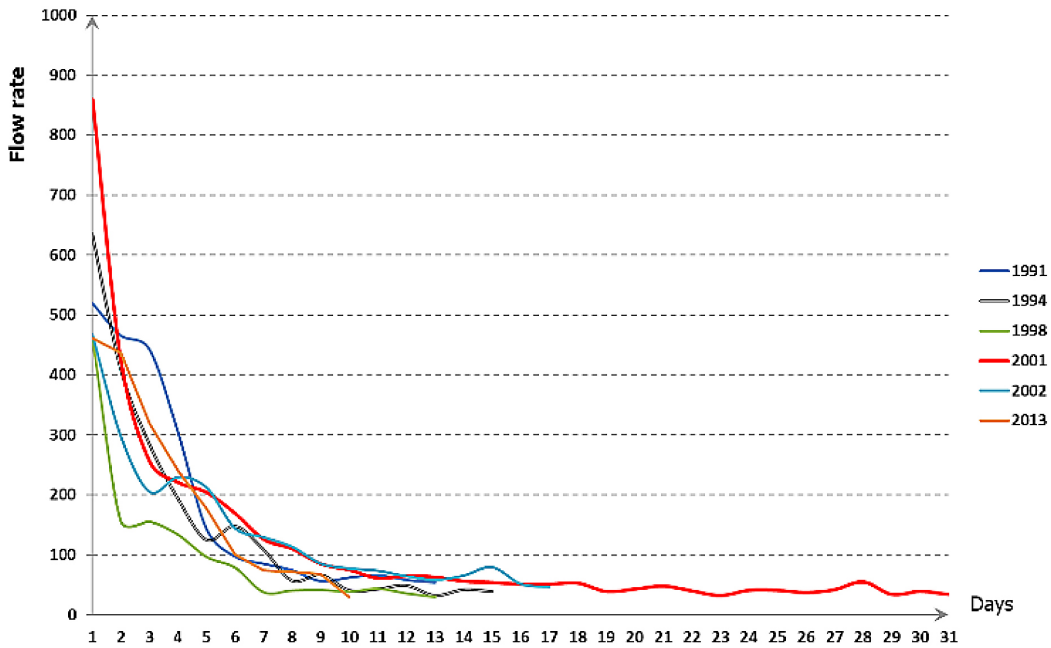


Figure 7. Different recession curves of the Ras El Ma Spring

zone), the function  $\varphi(t)$  is the function of the drying-off curve which corresponds to the emptying of the flooded area. Thus, the whole of the recession curve (Fig. 8) can be presented according to the following equation (Eq. 1):

$$Qt = \psi(t) + \varphi(t) \tag{1}$$

The dry-off curve is defined by the coefficient of Maillet’s emptying law [Ford and Williams, 2007], which is as follow (Eq. 2):

$$\varphi(t) = Q_{R0}e^{-\alpha t} \tag{2}$$

where:  $Q_{Rt}$  - the Drying flow rate at a time (t);  $Q_{R0}$  - the ordinate of the dry-off curve at  $t = 0$ ;  $t$  - represents time;  $\alpha$  - the drying-off coefficient, must be adjusted to the observed drying-off curve (Eq. 3).

$$\alpha = \frac{\log Q_{R0} - \log Q_{Rt}}{t} \tag{3}$$

In order to characterize the infiltration, Mangin [1975] suggests using the homographic function expressed by (Eq. 4).

$$\psi(t) = q_0 * \frac{(1 - \eta t)}{(1 + \varepsilon t)} \tag{4}$$

where:  $q_0$  is the difference between peak flow;  $Q_{t_0}$  and  $Q_{R_0}$ ;  $q_0 = Q_{t_0} - Q_{R_0}$ ;  $\eta = 1/t_i$  given in day-1 with  $[0, t_i]$  equal to the duration of the rapid decline;  $\eta$  is related to the infiltration speed, so the lower the

value of  $\eta$ , the slower the infiltration;  $\varepsilon$  is the coefficient of heterogeneity characterizing the type of groundwater circulation (Eq. 5).

$$\varepsilon = \frac{(q_0 - q_t)}{(q_t * t)} - \frac{\eta q_0}{q_t} \tag{5}$$

The total initial volume ( $V_t$ ) supplied by the source at  $t_0$  (flood peak) is the sum of the dynamic volume ( $V_{dyn}$ ) and the volume drained during the rapid decline ( $V^*$ ).

The dynamic volume ( $V_{dyn}$ ) expressed by equation (4) is calculated by integrating the equation (2)

$$V_{dyn} = \int_0^\infty Q_{R0}e^{-\alpha t} = C \frac{Q_{R0}}{\alpha} \tag{6}$$

The drained volume during the rapid recession ( $V_1^*$ ) is calculated by (Eq. 7)

$$V_1^* = \int_0^{t_i} q_0 \frac{(1 - \eta t)}{(1 + \varepsilon t)} dt = \frac{q_0}{\varepsilon} \left[ Ln(1 + \varepsilon t_i) \left( 1 + \frac{\eta}{\varepsilon} \right) - \eta t_i \right] \tag{7}$$

One of the objectives of this method is to be able to classify the different karstic systems based on their functioning. In order to simplify this classification, Mangin [1975] proposed the study of two dimensionless coefficients, ( $k$ ) and ( $i$ )

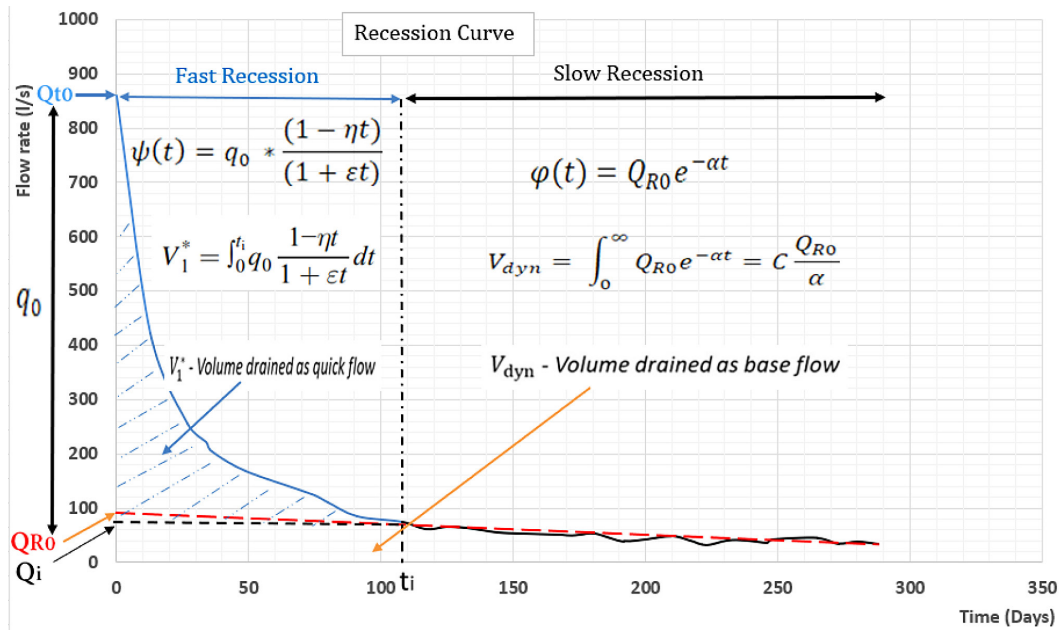


Figure 8. Recession curve of the Ras El Ma spring

relating to the functioning of the infiltration zone and to the volume of flooded karst, respectively.

These two coefficients defined as follows:

- 1)  $k$  is equal to the dimensionless ratio between the greatest dynamic volume value calculated over a large period and the interannual transit volume. This interannual transit volume corresponds to the volume passed over a large number of hydrological

cycles divided by the number of cycles considered. Thus,  $k$  reflects the ability of the system to store high water reserves in order to restore them during low flow, i.e. its regulatory power. In the case of karst aquifers,  $k$  is generally less than 0.5. A value close to zero indicates a low regulating power. On the other hand, a value which tends towards 1 implies significant reserves.

Table 1. Parameters from Mangin’s method (Mangin 1975, 1984) for Ras-Elma source for six recession periods

Parameters (Mangin’s method)	Units	R <sub>28/03/1991</sub>	R <sub>18/02/1994</sub>	R <sub>13/02/1998</sub>	R <sub>09/03/2001</sub>	R <sub>17/04/2002</sub>	R <sub>12/03/2014</sub>
$\psi(t)$ function							
$Q_{T_0}$	m <sup>3</sup> s <sup>-1</sup>	0.520	0.635	0.464	0.859	0.468	0.070
$\eta$	days <sup>-1</sup>	0.007	0.006	0.005	0.009	0.009	0.0054
$\epsilon$	days <sup>-1</sup>	0.006	0.0188	0.0213	0.034	0.0038	0.0099
$q_0$	m <sup>3</sup> /s	0.451	0.585	0.416	0.769	0.355	0.271
$\phi(t)$ function							
$Q_{R_0}$	m <sup>3</sup> s <sup>-1</sup>	0.069	0.050	0.048	0.090	0.113	0.341
$\alpha$	days <sup>-1</sup>	0.0003	0.0004	0.0002	0.0012	0.0024	0.0001
$Q_i$	m <sup>3</sup> s <sup>-1</sup>	0.056	0.041	0.038	0.075	0.058	0.042
$t_i$	days	148	157	216	108	110	185
Recession duration	days	241	242	325	288	164	215
Infiltration volume ( $V_1^*$ )	10 <sup>6</sup> m <sup>3</sup>	3.97	2.34	0.1	5.87	1.5	3.82
Dynamic volume ( $V_{dyn}$ )	10 <sup>6</sup> m <sup>3</sup>	5.89	10.8	20.73	6.48	4.068	0.6
Total initial volume ( $V_t$ )	10 <sup>6</sup> m <sup>3</sup>	9.86	13.14	20.83	10.45	5.56	4.42
$k = \frac{V_d}{V_t}$	-	0.59	0.82	0.99	0.62	0.73	0.13
$i = \frac{1 - \eta t}{1 + \epsilon t}$	-	0.97	0.96	0.97	0.92	0.97	0.96

2)  $i$  is equal to the dimensionless value that  $\psi(t)$  takes two days after the flood period. Thus, it reflects the speed of the karst system in transmitting rainfall information so it reflects the degree of karstification. The  $k$  and  $i$  indices are calculated by equations (8) and (9), respectively:

$$k = \frac{V_d}{V_r} \quad (8)$$

$$i = \frac{1 - \eta t}{1 + \varepsilon t} \quad (9)$$

The main results of this application are shown in the Table (1).

The quantitative characterization of the infiltration conditions in the unsaturated zone and the storage capacity of the saturated zone of the karstic aquifer relative to the source of Ras El Ma is demonstrated by the application of the Mangin's method [1975; 1984]. The hydrodynamic behavior and hydrological functioning of this aquifer will be concluded as follows:

From the results of the  $\psi(t)$  function, it can be seen that the recession is spread over four months, which may be due to a non-immediate response to the input signal (rain). The heterogeneity coefficient ( $\varepsilon$ ) and the infiltration coefficient ( $\eta$ ) are respectively of the order of 0.034  $J^{-1}$  and 0.009  $J^{-1}$  for the year 2001 taken as a reference for considerations already mentioned. These parameters indicate a not very marked concavity of the recession curve, which reflects less rapid declines than those observed in other karstic regions, especially in the dry period such as the Olhos de Água do Anços source in Portugal [Paiva and Cunha, 2020].

Moreover, the average value of the infiltration index  $i$  is 0.95 which is very close to 1. This leads to concluding that this karst system is complex, recharged by a slow or delayed infiltration contributing to a better flow regulation. This parameter thus confirms the observations already mentioned.

This system can be compared to the System of the Dir of Beni-Mellal in the Middle Atlas and that of the Imouzzer region of the Western High Atlas [Bouchaou, 1995 and Qurtobi 1996]. Another comparison can be made with another karst system in the Rif area, the hydrodynamic functioning of the Ras El Maa and Chrafate springs shows the presence of a very inertial, poorly drained and poorly karstified system [El Bardai, Targuisti and Aluni 2014].

In other words, the drying curve representing the function  $\phi(t)$  is characterized by a very

soft slope, which means that the volume of water stored in the saturated zone is higher causing the steady decrease in flow over time. The drying coefficient ( $\alpha = 0.0007 \text{days}^{-1}$ ) is low and suggests a very slow emptying of the reservoirs of which the calculated dynamic volumes are part. This considerable storage capacity of the Ras El Ma Karst Aquifer saturated zone can be explained by the Vauclisian characteristics of the saturated zone, which allows classifying this karst among this type. However, this conclusion remains hypothetical.

The second explanation relating to this storage capacity can be related to the structural characteristics already discussed in the first approach targeted by this study, which suggests supply from other panels guided by the fault network

The values of ( $k$ ) are important reflecting a regulating power of flows which is important and therefore, a little karst character of the drowned area of the spring. This is in line with the previous interpretations. However, this large storage capacity is responsible for the perennial nature of the Ras El Ma spring even in a very dry year.

According to the Mangin karst system classification diagram, as well as the ( $i$ ) and ( $k$ ) indices values, the aquifer studied here is in the field of poorly karstified systems with the exception of the values of the year 2014 that classifies the karst in a complex system. However, the values of the  $k$  parameter should be used with caution and the interpretation cannot be taken further, due to the limited number of outlets and recession curves having smaller measurement steps. In most karst aquifers, ( $k$ ) is generally less than 0.5, but in the case of Ras El Ma, with the exception of the year 2014, this parameter far exceeds the norm. Moreover, it is observed that the value of the infiltration index ( $i$ ) is relatively greater than 0.5.

Moreover, this classification remains equivocal; because this karst region is the area of all karst manifestations of surface as well as those of depth including a large number of caves, no less than 365, the most important is the cave of Friouato, 27 km from the city of Taza, around the national park of Tazekka. These karst manifestations testify to a karstification phenomenon of a greater order than that highlighted by these results.

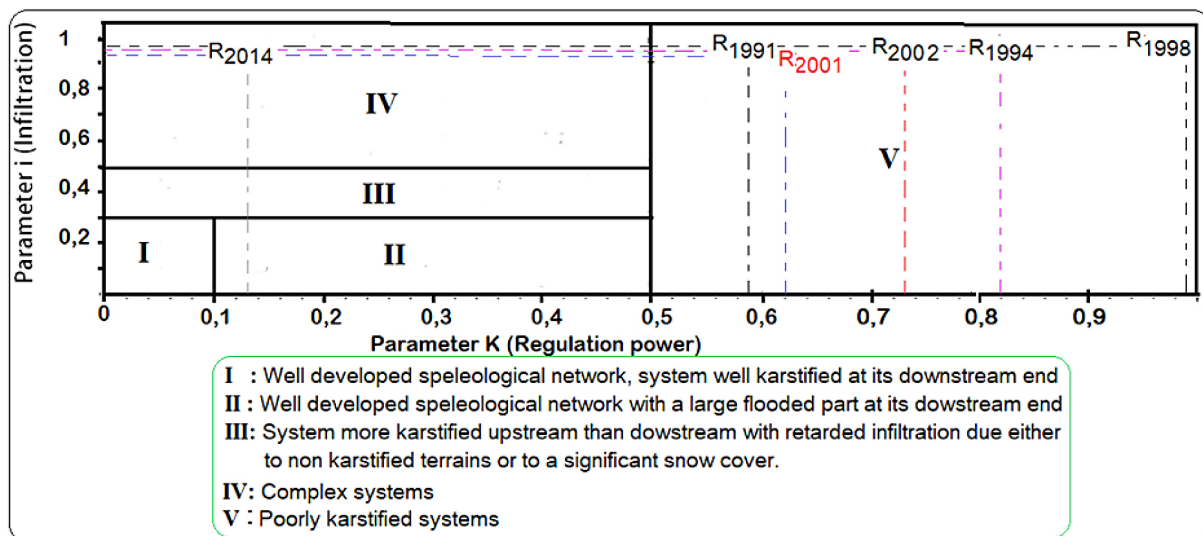


Figure 9. Classification of the Ras-Elma karst system in the Mangin (1975; 1984) diagram

### Contribution of hydrogeochemistry in understanding of karst functioning

#### *Evolution chronicle of the physicochemical composition of Ras El Ma spring waters*

The physico-chemical parameters characterizing a water, can undergo different seasonal variations. These variations related to the supply of a large volume of water, allow better understanding the functioning of the aquifer.

The evolution of these parameters follows the classical pattern described by some authors [Bakalowicz, 1979; Bouchaou, 1995; Paiva, 2020] in a karst environment, i.e., following a downpour, the water from the springs undergoes variations of temperature, of pH and mineralization. These variations will be a function of the abundance and intensity of rainfall. Thus, the magnitude of the temperature variation of the spring water depends on the importance of the recharge event and the previous hydraulic conditions of the system. The pH will also be influenced by these water temperature contrasts.

The temperature and the pH of the water of the Ras El Ma spring have an antagonistic evolution (Fig. 10). The average temperature variations (2 °C) indicate the existence of a slightly rapid circulation through a functional network of conduits and a concentrated recharge.

The pH of the waters of the karstic spring of Ras El Ma is basic, both in winter and summer. Thus, the calco-carbonic balance will not be much influenced and subsequently the attack of the carbonate casing will be weak. This finding is

consistent with the results proven by the hydrodynamic study, namely the low karstic character of the drowned area of the source

In Figure (10), low conductivity values are measured during rainy events (January) while high values are recorded at the end of February, in June, July, August and September.

The evolution of conductivity is closely related to that of ions ( $\text{HCO}_3^-$ ,  $\text{Mg}^{2+}$  and  $\text{Ca}^{2+}$ ). Indeed, the evolution of their respective curves follows a pace close to conductivity curve. Thus, low values during the rainy period and a tendency to a gradually increase during low water levels are noted. Adversely, the ion contents ( $\text{Cl}^-$ ,  $\text{Na}^+$  and  $\text{K}^+$ ) increase during the rainy season and tend towards a decrease in low water levels. Their origin refers to Triassic marls and gypsiferous clays rich in salts (halite).

The physico-chemical water behavior of the Ras Elma spring reflects its conditions of emergence. The contents of  $\text{HCO}_3^-$ ,  $\text{Mg}^{2+}$  and  $\text{Ca}^{2+}$  come from the Liassic limestones, the major facies from which this source is issued. The Triassic salt and gypsiferous soils, which constitute the sealing facies either at the base of the aquifer or of the boundaries between the hydrological panels inherited by structural compartmentalization, provide  $\text{SO}_4^{2-}$ ,  $\text{Na}^+$  and  $\text{Cl}^-$  ions. These elements are abundant in high water periods by leaching of these evaporitic facies.

#### *Contribution of water chemistry to understanding the karstogenesis phenomena*

In the previous paragraph it was noted that the variation in water inputs to carbonate aquifers automatically implies variations in the

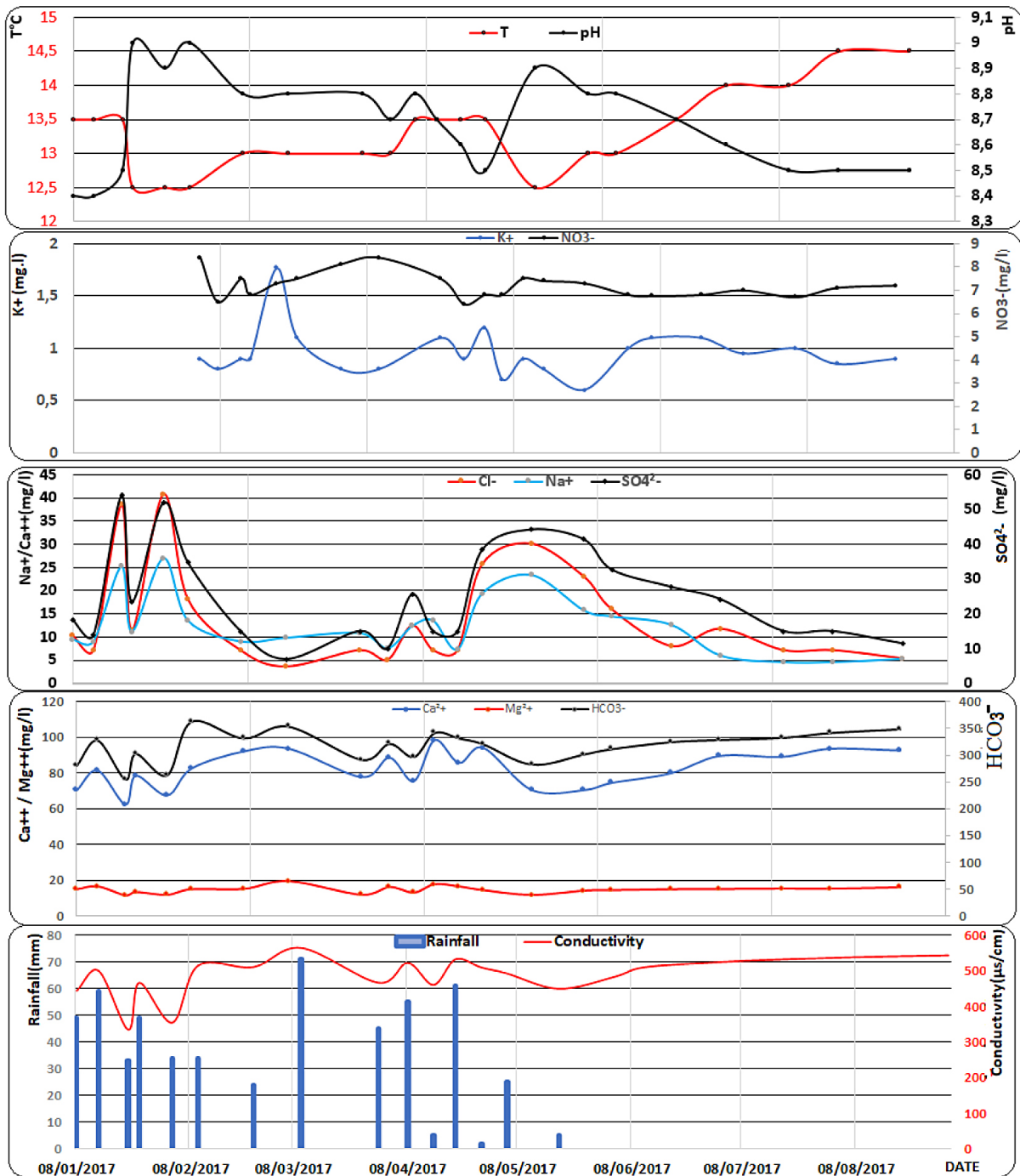


Figure 10. Evolution chronicle of the physicochemical composition of the water of Ras El Ma

concentrations of chemical elements during the different seasons. This let wondering about the consequences of such phenomena on the evolution of karst formation (karstogenesis).

Changes in the conditions of inflow (rain) and outflow (source flow) of aquifers due to increased water volumes generally result in an increase in the flow rate in the internal areas of the karst (Couturaud, 1993). This phenomenon implies new possibilities for increased karstification,

either by underground erosion or by the rapid arrival of water that remains corrosive at depth.

Indeed, the supply of a large amount of new and aggressive water from the superficial sectors will dissolve the carbonate rock and this in deep in the system. This water must be enriched with  $CO_2$ , because it stays momentarily in the epikarst so close to the ground, area of production of this gas.

This water will be less saturated with respect to calcite compared to the water before the rainy episode, by the fact that its residence time in the

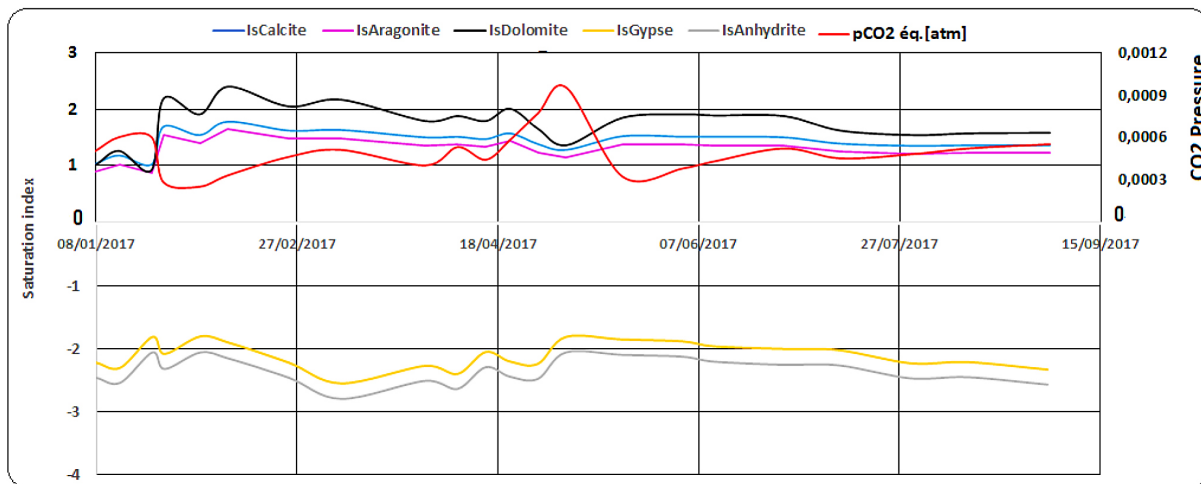


**Figure 11.** Evolution Chronicle of different phases of mineralization in relation to CO<sub>2</sub> pressure

epikarst has not been long enough and that the contact with the carbonate rock is less important too.

The analysis of the CO<sub>2</sub> pressure parameter (pCO<sub>2</sub>), calculated from the Wateq Software, essentially shows a significant peak in April and a significant decrease in saturation indices (Fig. 11). The saturation indices of the waters of this source calculated in relation to different phases of mineralization show that these waters are oversaturated compared to aragonite, calcite and dolomite, but they are undersaturated with respect to gypsum and anhydrite. These mineral phases are characteristic of highly outcropping carbonate rocks in the study area. Even in the presence of rains during January and March, pCO<sub>2</sub> remained low reflecting that the carbonates dissolution phenomenon was present but in small quantities. Conversely, as soon as the rains of April arrived, a stronger increase in the pCO<sub>2</sub> was noted compared to the other months, and a greater decrease in the value of saturation indices of calcite, aragonite and dolomite. Furthermore, there is a slight increase in the saturation indices of gypsum and anhydrite.

The difference in behavior of pCO<sub>2</sub> between the January and March, and April can be explained by the intense regrowth of vegetation during this month (full spring). This vegetation remains the origin of this gas export of to the epikarstic zone.

It should also be noted that the low value recorded for the saturation indices of calcite, aragonite and dolomite are due to the fact that the infiltrated waters remained much more in the epikarstic zone than at the level of the drowned zone already filled by the waters of previous events (January and March). In addition, the evolution of gypsum saturation indices and anhydrite are independent

of pCO<sub>2</sub>, because they are directly related to the dissolution of the evaporites of the crossed Triassic formation, which constitute the sealing facies either at the base of the aquifer or of the boundaries between the hydrological panels inherited by structural compartmentalization already mentioned.

## CONCLUSIONS

The study of the karst hydrodynamic behavior in the southwest of Taza shows certain cyclicity in the Ras El Ma flow variations at the interannual scale. Flood hydrographs reveal two variation types, uni-modal which usually occurs following rainfall concentrated in time and a second multi-modal type repetitive rainfall in the basin.

Modeling by using the Mangin method of the recession curve for the year 2001 taken as a reference highlights that the karst system is complex or even poorly karstified, according to the values of different coefficients and indices. The coefficient of heterogeneity  $\varepsilon = 0.034 \text{ days}^{-1}$ , the infiltration coefficient  $\eta = 0.009 \text{ days}^{-1}$ , the drying coefficient  $\alpha = 0.0007 \text{ days}^{-1}$ , the infiltration index  $i = 0.92$  and the regulatory power index  $k = 0.62$ .

The physico-chemical behavior of the Ras El Ma spring reflects its conditions of emergence. Accordingly, the HCO<sub>3</sub><sup>-</sup>, Mg<sup>2+</sup> and Ca<sup>2+</sup> contents come from the Liassic limestones. The salt and gypsiferous soils are from Triassic, which constitute the sealing facies either at the aquifer basement or at the boundaries between the hydrological panels inherited by structural compartmentalization, providing SO<sub>4</sub><sup>2-</sup>, Na<sup>+</sup> and Cl<sup>-</sup>. These elements are abundant in high water periods by leaching the Triassic evaporitic rocks.

## REFERENCES

1. Anderson M.P. 2005. Heat as a ground water tracer. *Groundwater*, 43(6), 951–968.
2. Andreo B., Vías J., Durán J., Jiménez P., López-Geta J., Carrasco F. 2008. Methodology for groundwater recharge assessment in carbonate aquifers: application to pilot sites in southern Spain. *Hydrogeology Journal*, 16(5), 911–925.
3. Auajjar J., Boulegue J. 1999. Les minéralisations Pb-Zn (Cu) Ba du district du Tazekka (Taza, Maroc oriental), chronique de la recherche minière, 536–537, 121–135.
4. Bakalowicz M. 2008. in Paiva I., Cunha L. 2020. The karst environment: studies and perspectives, identification and characterization of the resource. Proceedings of the technical days of the French Committee of the International Association of Hydrogeologists Hydrogeology and Karst through work of Michel Lepiller, Université d'Orléans, Orléans, France, 11–27.
5. Bakalowicz M. 2005. in Paiva I., Cunha L. 2020. Karst groundwater: a challenge for new resources. *Hydrogeology Journal*, 13, 148–160.
6. Bakalowicz M. 1999. Extrait de Connaissance et gestion des ressources souterraines en eaux souterraines dans les régions karstiques, guide technique n° 3, SDAGE Rhône-Méditerranée-Corse, 40.
7. Benshili K. 1989. Lias dogger du moyen Atlas plissé (Maroc). Sédimentologie, biostratigraphie et évolution paléogéographique. PhD Thesis, Université de Lyon, 106.
8. Bérard P. 1982. Interprétation des images satellites en complément à la photo-interprétation traditionnelle pour la définition des structures hydro-géologiques au Niger et en Haute-Volta, Colloque sur les milieux discontinus en hydrogéologie, Bureau de recherches géologiques et minières, Orléans. 67–82.
9. Bicalho C., Batiot-Guilhe C., Deidel JL., Van Exter S., Jourde H. 2012. Geochemical evidence of water source characterization and hydrodynamic responses in a karst aquifer. *Journal of Hydrology*, 450–451, 206–218.
10. Birk S., Liedl R., Sauter M. 2004. Identification of localized recharge and conduit flow by combined analysis of hydraulic and physicochemical spring responses (Urenbrunnen, SW-Germany). *Journal of Hydrology*, 286, 179–193.
11. Bonacci O. 1993. Karst spring hydrographs as indicators of karst aquifers. *Hydrological sciences journal*, 38, 51–62.
12. Bouchaou L. 1995. Fonctionnement des aquifères atlasiques et leur relation avec les aquifères de la plaine : Cas de l'atlas de béni Mellal et de la plaine de Tadla. PhD Thesis, Université Cadi Ayyad, Marrakech (Maroc).
13. Chang Y., Wu J., Liu L. 2015. Effects of the conduit network on the spring hydrograph of the karst aquifer. *Journal of Hydrology*, 527, 517–530.
14. Combe M. 1977. Ressources en eaux du Maroc. Domaine Atlasique sud atlasique. Notes et mémoires du service géologique du Maroc, 433.
15. Colo G. 1961. Contribution à l'étude du Jurassique du Moyen Atlas septentrional. Notes et mémoires du service géologique du Maroc, 139.
16. Couturaud A. 1993. Hydrogéologie de la partie occidentale du système karstique de Vaucluse, Thèse de doctorat, Université d'Avignon, 159.
17. El Bardai R., Targuisti K., Aluni K. 2014. Caractérisation hydrodynamique des sources karstiques : cas de la source de Ras El Maa (Rif Septentrional, Maroc). *Revue des sciences de l'eau, Journal of Water Science*, 27(2), 139–153.
18. Fiorillo F. 2014. The recession of spring hydrographs focused on karst aquifers. *Water Resource Management*, 28(7), 1781–1805.
19. Fiorillo F. 2011. Tank-reservoir drainage as a simulation of recession limb of karst spring hydrographs. *Hydrogeology Journal*, 19, 1009–1019.
20. Florea L., Vacher H. 2006. Springflow hydrographs: eogenetic vs. telogenetic karst. *Groundwater*, 44(3), 352–361.
21. Ford D., Williams P. 2007. Karst hydrogeology and geomorphology. Wiley, Chichester, UK, 562.
22. Frizon de Lamotte D., Crespo-Blanc A., Saint-Bezar B., Comas M., Fernandez M., Zeyen H., Ayarza H., Robert-Charrue C., Chalouan A., Zizi M., Teixell A., Arboleya M.L., Alvarez-Lobato F., Julivert M., Michard A. 2004. Transmed-transect I [Betics, Alboran Sea, Rif, Moroccan Méseta, High Atlas, Jbel Saghro, Tindouf basin], in: W. Cavazza, F. Roure, W. Spakman, G.M. Stampfli and P.A. Ziegler (Eds), *The Transmed Atlas – the Mediterranean region from crust to mantle*, Springer, Berlin.
23. Gárfias-Soliz J., Llanos-Acebo H., Martel R. 2010. Time series and stochastic analysis to study the hydrodynamic characteristics of karst aquifers. *Hydrological Process*, 24, 300–316.
24. Ghasemizadeh R., Hellweger F., Butscher C., Padilla I., Vesper D., Malcolm F., Alshawabkeh A. 2012. Review: Groundwater flow and transport modeling of karst aquifers, with particular reference to the north coast limestone aquifer system of Puerto Rico. *Hydrogeology Journal*, 20(8), 1441–1461.
25. Gil-Márquez J., Andreo B., Mudarra M. 2019. Combining hydrodynamics, hydrochemistry, and environmental isotopes to understand the hydrogeological functioning of evaporite-karst springs: an example from southern Spain. *Journal of Hydrology*, 576, 299–314.

26. Goldscheider N, Drew D. 2007. Methods in karst hydrogeology. IAH International Contributions to Hydrogeology, 26, 264.
27. Hartmann A., Goldscheider N., Wagener T., Lange J., Weiler M. 2014. Karst water resources in a changing world: Review of hydrological modeling approaches. 52, 218–242.
28. Jukić D., Denić-Jukić V. 2011. Partial spectral analysis of hydrological time series. Journal of Hydrology, 400, 223–233.
29. Kovács A., Perrochet P., Király K., Jeannin P-Y. 2005. A quantitative method for the characterization of karst aquifers based on spring hydrograph analysis. Journal of Hydrology, 303, 152–164.
30. Kresic N., Stevanovic Z. 2010. Groundwater hydrology of springs. Engineering, theory, management, and sustainability. Butterworth Heinemann, Oxford, 573.
31. Labat D., Ababou R., Mangin A. 2000. Rainfall-runoff relations for karstic springs, part I: convolution and spectral analysis. Journal of Hydrology, 238(3–4), 123–148.
32. Liñan C., Andreo B., Mudry J., Carrasco Santos F. 2009. Groundwater temperature and electrical conductivity as tools to characterize flow patterns in carbonate aquifers: the Sierra de las Nieves karst aquifer, southern Spain. Hydrogeology Journal, 17, 843–853.
33. Laville E., Piqué A., Amrhar M., Charroud M. 2004. A restatement of the Mesozoic Atlasic Rifting (Morocco). Journal of African Earth Sciences, 38(2), 145–153.
34. Laville E., Faden B. 1989. The Moroccan Atlasic system in the Jurassic: Structural evolution and geodynamic framework]. Sciences Géologiques, bulletins et mémoires, 84, 3–28.
35. Liu L., Shu L., Chen X., Oromo T. 2010. The hydrologic function and behavior of the Houzhai underground river basin, Guizhou Province, southwestern China. Hydrogeology Journal, 18, 509–518.
36. Luhmann A.J. 2011. Water temperature as a tracer in karst aquifers. PhD Thesis, University of Minnesota, Minneapolis, MN, 164.
37. Malík P., Vojtková S. 2012. Use of recession-curve analysis for estimation of karstification degree and its application in assessing overflow/underflow conditions in closely spaced karstic springs. Environmental earth sciences, 65(8), 2245–2257.
38. Mangin A. 1984. For a better understanding of hydrological system from correlation and spectral analyses. Journal of Hydrology, 67, 25–43
39. Mangin A. 1975. Contribution to the hydrodynamic study of karst aquifers. Thèse de doctorat. Université de Dijon (France). (in French)
40. Mathieu L., EK C. 1964. The Daia Chikker: Geomorphological study. Annals of the Geological Society of Belgium, 87(15), 65–103.
41. Martínez-Santos P., Andreu J. 2010. Lumped and distributed approaches to model natural recharge in semiarid karst aquifers. Journal of Hydrology, 388(3–4), 389–398.
42. Massei N., Mahler B.J., Bakalowicz M., Fournier M., DuPont J.P. 2007. Quantitative interpretation of conductivity frequency distributions in karst. Groundwater, 45(3), 288–293.
43. Mikszewski A., Kresic N. 2015. Mathematical modeling of karst aquifers. In: Stevanovic Z (ed) Karst aquifers: characterization and engineering. Springer, Cham, Switzerland, 283–298.
44. Naoura J. 2012. Hydrological and qualitative characterization of surface water in the Upper Inaouene watershed, PhD thesis, Université Sidi Mohamed Ben Abdellah, Fès (Maroc).
45. Paiva I., Cunha L. 2020. Characterization of the hydrodynamic functioning of the Degraças-Sicó Karst Aquifer, Portugal. Hydrogeology Journal 28, 2613–2629.
46. Panagopoulos G., Lambrakis N. 2006. The contribution of time series analysis to the study of the hydrodynamic characteristics of the karst systems: application on two typical karst aquifers of Greece, Trifilia, Almyros Crete. Journal of Hydrology, 329, 368–376.
47. Petalas C., Akratos C., Tsihrintzis V. 2018. Hydrogeological investigation of a karst aquifer system. Environmental Processes, 5(1), 155–18.
48. Rachid A. 1997. The Neogene basins of the southern Rifian trench and the north eastern Rif (Morocco). Sedimentology, paleogeography and dynamic evolution. State thesis. Univ. Sidi Mohamed Ben Abdellah, Fès., 333.
49. Rahnemaei M., Zare M., Nematollahi A.R., Sedghi H. 2005. Application of spectral analysis of daily water level and spring discharge hydrographs data for comparing physical characteristics of karstic aquifers. Journal of Hydrology, 311, 106–116.
50. Ramirez Merino J.I., Portero G., Aït Brahim L., Chalouan A., Hoepffner Ch., Tahiri ELousrouti M. 2008. Notes and memoirs of the geological service n° 433 bis for the sheet of Taza, national plan of geological cartography, editions of the geological service of Morocco.
51. Rehr C., Birk S. 2010. Hydrogeological characterisation and modelling of spring catchments in a changing environment. Austrian Journal of Earth Sciences, 103(2), 106–117.
52. Robillard D. 1981. Étude stratigraphique et structurale du moyen Atlas septentrional (région de Taza, Maroc). Notes et mémoires du service géologique, 308, 101–193.
53. Robillard D. 1979. Tectonique syn-sédimentaire du Moyen Atlas septentrional au sud de Taza, Maroc. Thèse de doctorat, Université des sciences et techniques de Lille (France).
54. Rodier J. 1980. L'analyse de l'eau. 6<sup>ème</sup> Ed. Dunod.

55. Sánchez D., Barberá J.A., Mudarra M., Andreo B. 2015. Hydrogeochemical tools applied to the study of carbonate aquifers: examples from some karst systems of southern Spain. *Environmental earth sciences*, 74, 199–215.
56. Sabaoui A. 1998. Rôle des inversions dans l'évolution méso-cénozoïques du Moyen Atlas septentrional (Maroc). L'exemple de la transversale ElManzel-Ribat, ElKhayr-Bou Iblane. Thèse d'état, Univ. Mohamed V. Rabat, 432.
57. Taylor C., Greene E. 2008. Hydrogeologic characterization and methods used in the investigation of karst hydrology. In: Rosenberry D., LaBaugh J. (eds) *Field techniques for estimating water fluxes between surface water and ground water*. US Geological Survey, Reston, VA, 75–114.
58. Wang Z., Chen Q., Yan Z., Luo M., Zhou H., Liu W. 2019. Method for identifying and estimating karst groundwater runoff components based on the frequency distributions of conductivity and discharge. *Water*, 11(12), 2494.
59. White W. 1988. *Geomorphology and hydrology of karst terrains*. Oxford University Press, New York, 464.